Comments on Inorganic Chemistry
Publication details, including instructions for authors and subscription information:
http://www.informaworld.com/smpp/title~content=t713455155

Dynamic Processes in the Lowest-Excited ^{3}MLCT States of $[M(L)_{3-x}(L')_x]^2$ (L,L' = diimine; M = Ru,Os)

H. Riesen[a]; E. Krausz[a]
[a] Research School of Chemistry The Australian National University, Canberra, Australia

To cite this Article Riesen, H. and Krausz, E.(1995) 'Dynamic Processes in the Lowest-Excited ^{3}MLCT States of $[M(L)_{3-x}(L')_x]^2$ (L,L' = diimine; M = Ru,Os)', Comments on Inorganic Chemistry, 18: 1, 27 — 63
To link to this Article: DOI: 10.1080/02603599508033862
URL: http://dx.doi.org/10.1080/02603599508033862

Dynamic Processes in the Lowest-Excited ^{3}MLCT States of $[M(L)_{3-x}(L')_x]^{2+}$ (L,L' = diimine; M = Ru,Os)

H. RIESEN and E. KRAUSZ
Research School of Chemistry
The Australian National University,
Canberra, ACT 0200, Australia

A clear understanding of the lowest-excited ^{3}MLCT states of $[Ru(bpy)_3]^{2+}$ and related systems in crystalline hosts of well-defined symmetry is outlined, based on a range of incisive experiments such as Zeeman, Stark, line narrowing and spectral hole-burning measurements. The lowest-excited ^{3}MLCT states of ruthenium complexes are localised. The intramolecular excitation energy transfer can be relatively slow ($\approx$10 ns). In the $[Os(bpy)_3]^{2+}$ complex analogous excitations are well described as coherent intramolecular excitons. Cases are found in which the small effect associated with selective deuteration leads to exciton localisation. The influence of nanoheterogeneity in solutions and glasses gives rise to a substantial inequivalence of the ligands, invariably leading to localization.

Key Words: *charge transfer states, localisation, excitation exchange interactions, intramolecular excitons, Stark, Zeeman, luminescence line narrowing, excitation line narrowing, spectral hole-burning*

1. INTRODUCTION

The properties of the lowest-excited triplet metal-to-ligand charge transfer (^{3}MLCT) states of $[Ru(bpy)_3]^{2+}$ and $[Os(bpy)_3]^{2+}$ have been

Comments Inorg. Chem.
1995, Vol. 18, No. 1, pp. 27–63
Reprints available directly from the publisher
Photocopying permitted by license only

the subject of a large number of reviews over the last two decades.[1–6] The question whether the transferred electron in these states is localised or delocalised was often addressed.

It is now accepted[7–12] that the lowest-excited ^{3}MLCT states in solutions and frozen glasses are localised. Compelling evidence was obtained from excited state resonance Raman (ERR) work.[7,8] For example, the same frequencies were observed[8] for the complexes *fac*-$XRe(CO)_3(bpy)$ with X = Cl or Br as for $[Ru(bpy)_3]^{2+}$. Also, the same ERR spectrum was observed in frozen glasses.[13,14] Thus the localisation in solutions cannot be caused by a solvent relaxation process.

The broadening of MLCT transitions in solutions and glasses is at least 500 cm^{-1}. In an amorphous medium each chromophore has a different environment (inhomogeneous broadening). Furthermore, the environment of each of the three ligands in a $[M(L)_3]$ complex is distinct (this is termed nanoheterogeneity in the following), and thus the MLCT excitation energies of the three ligands are generally inequivalent.

In solutions and glasses the average excitation exchange interaction between metal-ligand subunits must be less than the energy variations caused by the nanoheterogeneity; otherwise the electron would be delocalised. Thus it follows that the excitation exchange interaction in both $[Ru(bpy)_3]^{2+}$ and $[Os(bpy)_3]^{2+}$ must be less than 500 cm^{-1}. Such coupling between metal-ligand subunits (M-L) of a $[ML_3]^{2+}$ complex can be described by an exciton formalism.[15–17] The basis functions for an intramolecular exciton description (in the absence of vibronic coupling) are given in Eq. (1) where the asterisk denotes the excited M-L subunit. ϕ_i is the wavefunction of the metal-ligand subunit i.

$$\Phi_1 = |\phi_1^*\phi_2\phi_3|, \quad \Phi_2 = |\phi_1\phi_2^*\phi_3|, \quad \Phi_3 = |\phi_1\phi_2\phi_3^*|. \qquad (1)$$

The secular Eq. (2) is then obtained:

$$\begin{vmatrix} \epsilon_1 - \lambda & \beta & \beta \\ \beta & \epsilon_2 - \lambda & \beta \\ \beta & \beta & \epsilon_3 - \lambda \end{vmatrix} = 0. \qquad (2)$$

In Eq. (2) β is the excitation exchange interaction and ϵ_i is the

energy at zero interaction of the individual M-L subunit i. When there is no nanoheterogeneity (i.e., the three ligands are identical), the following eigenvectors and eigenvalues are obtained:

$$\Psi_A = 1/\sqrt{3}(\Phi_1 + \Phi_2 + \Phi_3) \quad \text{with energy } \epsilon + 2\beta, \tag{3}$$

$$\Psi_{E\pm} = \frac{-}{+} 1/\sqrt{3}(\Phi_1 + e^{\pm i2\pi/3}\Phi_2 + e^{\pm i4\pi/3}\Phi_3)$$

$$\text{with energy } \epsilon - \beta. \tag{4}$$

The subscripts A and $E_\pm$ denote the irreducible representations in the D_3 point group.

In solutions and glasses the energies ϵ_i will vary substantially due to the nanoheterogeneity. For localisation to occur the average of the energy differences $\epsilon_i - \epsilon_j$ must be larger than β.

We have used selective deuteration as a way to slightly alter the value of ϵ_i. Deuteration of a ligand i shifts the energy ϵ_i of this ligand to higher energy by Δ. For example, if $\Delta >> \beta$ the lowest-energy exciton becomes localised on the one protonated ligand if the other two ligands are deuterated. When $\beta \approx \Delta$, partial deuteration will not lead to localisation, but the lowest-energy exciton component will gradually shift to higher energy.

When coupling occurs between two ligands only, the secular equation is simply given by Eq. (5):

$$\begin{vmatrix} \Phi_1 & \Phi_2 \\ \epsilon_1 - \lambda & \beta \\ \beta & \epsilon_2 - \lambda \end{vmatrix} = 0 \tag{5}$$

with the following eigenvalues $\lambda_{1,2}$ and eigenvectors Ψ_1, Ψ_2:

$$\lambda_{1,2} = \frac{\epsilon_1 + \epsilon_2}{2} \pm \frac{\sqrt{(\epsilon_1 - \epsilon_2)^2 + 4\beta^2}}{2}, \tag{6}$$

$$\Psi_1 = \cos(\gamma)\Phi_1 + \sin(\gamma)\Phi_2,$$
$$\Psi_2 = \sin(\gamma)\Phi_1 - \cos(\gamma)\Phi_2 \tag{7}$$

where $\tan(2\gamma) = 2\beta/(\epsilon_2 - \epsilon_1)$

Of critical importance in the development of our present understanding of these systems has been the application of laser spectroscopies. Readers who would like to become more familiar with the power of these techniques are referred to our recent Comment[18] which provides a simple introduction to the field.

2. IMPORTANT CRYSTAL STRUCTURES

2.1 $[Ru(bpy)_3](PF_6)_2$

At room temperature $[Ru(bpy)_3](PF_6)_2$ crystallises in the trigonal space group $P\bar{3}c1$, preserving the inherent D_3-32 symmetry with only one D_3 site for the cation.[19] Between room temperature and 190 K a phase change to the space group P31 occurs and the unit cell triples. The structural modulation consists of small relative rotations of the cations about their threefold axis giving rise to three trigonal sites of C_3-3 symmetry.[20]

2.2 $[M(bpy)_3](ClO_4)_2$ (M = Zn, Ru)

Racemic $[M(bpy)_3](ClO_4)_2$ (M = Zn and Ru) crystallises in the monoclinic space group C2/c with four formula units per unit cell.[21,22] The structure can be described as a commensurate modulation of an idealised structure of $P\bar{3}c1$. All cations are equivalent and their symmetry is C_2-2. Within a single cation one ligand lies on the symmetry axis (= crystal *b* axis) while the other two ligands are equivalent. The two halves of each of these latter ligands are no longer equivalent. Bite angles and bond lengths are very similar for all three ligands, but the distinct ligand on the crystal *b* axis has a different anion environment. As a consequence, MLCT transitions to the distinct ligand lie several hundred wavenumbers higher in energy than corresponding transitions involving the crystallographically equivalent ligands. An energy difference of $\approx$2000 cm^{-1} is calculated by a simple point charge model in the $[Ru(bpy)_3](ClO_4)_2$ host.[23] The inequivalence of the ligands manifests itself in a substantial dichroism in the metal-ligand plane.[21]

The unit cell dimensions of a single crystal of $[Zn(bpy)_3](ClO_4)_2$ taken at 170 K confirm that no phase change occurs by this tempera-

ture.[21] The C2/c perchlorate salts have already locked into a modulated structure at room temperature, in contrast to the PF_6 salt.

3. PROBING THE C2/c CRYSTAL STRUCTURE

3.1 The Inequivalence of the Ligands

An important consequence of the C2/2 symmetry of this lattice is that complexes $[M(bpy)_{3-x}(L')_x]^{2+}$ with x = 1, 2 (M = Ru, Os; L' = bpy-d_8 and ligands similar to bpy, e.g., 3,3'-bipyridazine) can substitute the $[M(bpy)_3]^{2+}$ cation in the $[M(bpy)_3](ClO_4)_2$ host (M = Zn, Ru) in the two ways shown in Fig. 1.

The inequivalence of the ligands in the C2/c crystal structure of $[Zn(bpy)_3](ClO_4)_2$ can be probed by luminescence spectroscopy of

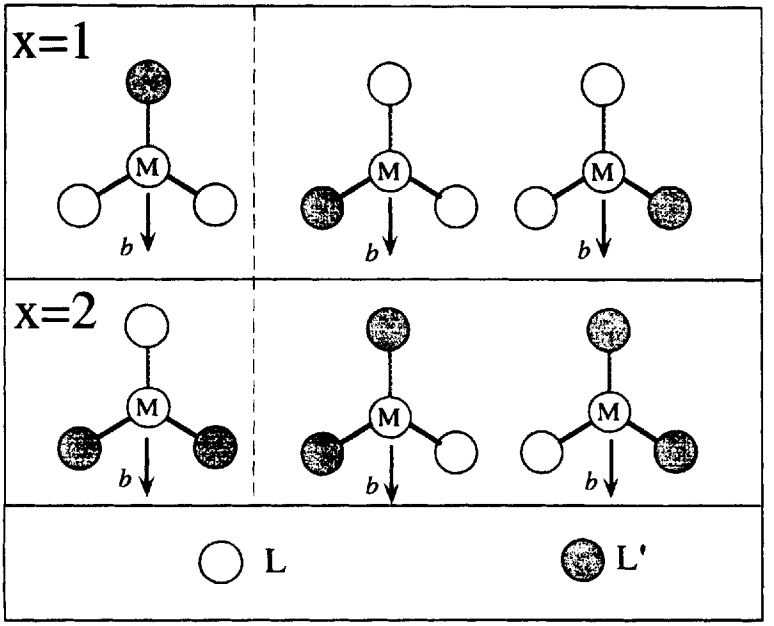

FIGURE 1 The two ways by which $[M(bpy)_{3-x}(L')_x]^{2+}$ complexes with x = 1 or 2 (L = bpy-d_8, bprid, etc.) can substitute $[Zn(bpy)_3]^{2+}$ in the $[Zn(bpy)_3](ClO_4)_2$ lattice. The crystal *b* axis is indicated.

suitable dopants. Such probes are provided by the $[M(bpy)_2(bprid)]^{2+}$ (M = Ru, Os; bprid = 3,3′-bipyridazine) complexes.[24] MLCT transitions to the bprid ligand are several thousand wavenumbers lower in energy than corresponding transitions involving the bpy ligand.[25] The ^{3}MLCT emission consists of two overlapping spectra. These arise from the bprid ligand in the two possible positions provided by the host.

The energy difference between the ^{3}MLCT transitions involving the bprid ligand in these two positions can then be directly determined.[24] We have observed differences of $\approx$360 cm^{-1} and $\approx$600 cm^{-1} for the bprid ligand in the ruthenium[24] and osmium[26] complex, respectively. The observed intensity ratio shows that the distinct position is at higher energy, in agreement with the point charge model. A simple point charge model characteristically overestimates energy differences. Furthermore, this calculation was performed for the $[Ru(bpy)_3](ClO_4)_2$ material.[23] It can be expected that the metal-ligand distances are somewhat different for the bprid ligand.

Intramolecular excitation energy transfer ensures that the $[Ru(bpy)(bprid)_2]^{2+}$ complex in the $[Zn(bpy)_3](ClO_4)_2$ lattice only emits[24] from a bprid ligand in one of the crystallographically equivalent positions (as there is inevitably a bprid in this position).

In the absence of knowledge of the crystal structure, Schmidt *et al.*[27] published spectra of the $[Ru(bpy)_2(2,2'\text{-bipyrazine})]^{2+}$ complex in the $[Zn(bpy)_3](ClO_4)_2$ host. They observed emissions with an intensity ratio of $\approx$1:2 separated by $\approx$260 cm^{-1}. They attributed these two emissions to two crystallographically distinct sites, but by analogy to the bprid case above, they are simply due to the two positions for the 2,2′-bipyrazine ligand.

3.2 Nanoheterogeneity of the Crystallographically Equivalent Ligands

In Fig. 2 excitation and luminescence spectra of the series $[Ru(bpy)_{3-x}(bprid)_x]^{2+}$ (x = 1 to 3) in the $[Zn(bpy)_3](ClO_4)_2$ host are shown in the region of the lowest-excited ^{3}MLCT origins I, II and III. The general pattern remains intact throughout the entire series. Note that dramatic variations would occur if the excitation exchange interaction β was larger than the inhomogeneous broadening of the electronic origins.

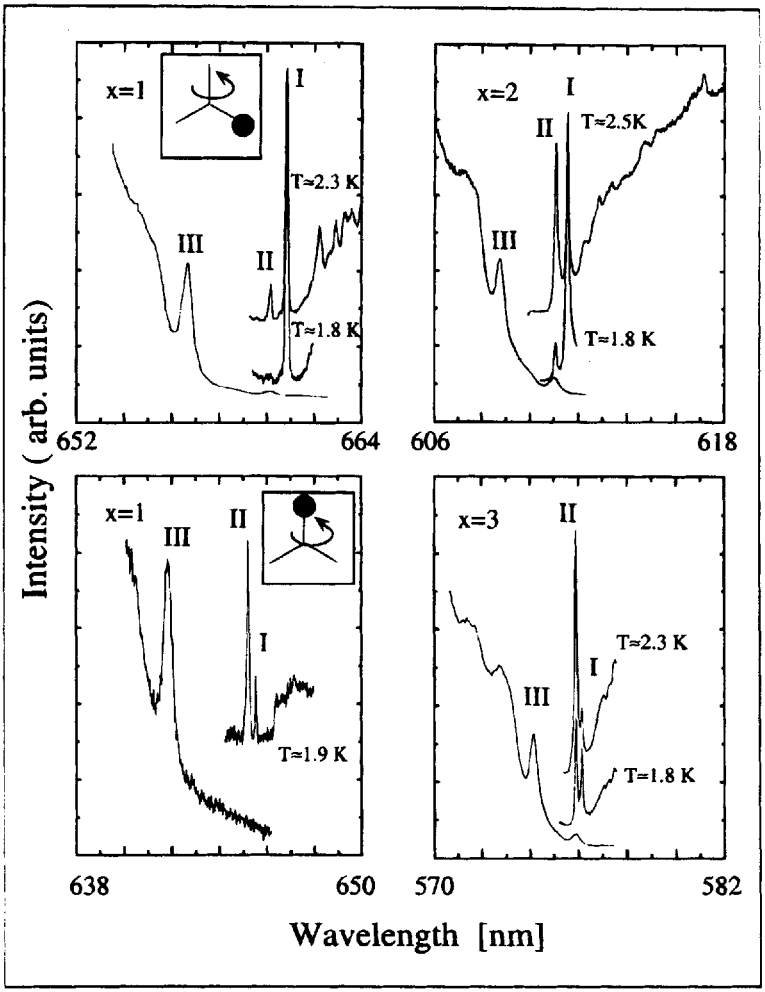

FIGURE 2 Excitation and luminescence spectra of the series $[Ru(bpy)_{3-x}(bprid)_x]^{2+}$ (x = 1 to 3) in $[Zn(bpy)_3](ClO_4)_2$ at low temperatures. The luminescence spectra were excited at the maxima of the origin III. The ligand position for the bprid ligand with respect to the twofold *b* axis is indicated for the two x = 1 spectra (Ref. 24.)

Laser selective spectroscopies establish that the transition energies of I, II and III are well correlated on each metal-ligand subunit. However, these transitions are poorly correlated amongst the metal-ligand subunits as a direct consequence of nanoheterogeneity. The inhomogeneous distributions of electronic origins involving the two crystallographically equivalent ligands are independent, i.e., for a particular energy of an origin involving one of the ligands the energy of the corresponding transition involving the ligand in the crystallographically equivalent position can be anywhere within the inhomogeneous distribution.

Figure 3 schematically portrays an excitation line narrowing experiment at lowest temperature. A small subsection of the inhomogeneously broadened emission (e.g., origin I) of ligand A is monitored. Origins I_A, II_A and III_A are narrowed as a consequence of the correlation of I-II and I-III spacings on one subunit.

In addition, broad features arise from excitation of the ligand B in the crystallographically equivalent position. After primary excitation, this metal-ligand B subunit can be deactivated by fast intramolecular energy transfer when the metal-ligand A subunit is at lower energy. The shaded distributions in Fig. 3 show the energies of such deactivated metal-ligand B subunits.

Simulations of excitation line narrowing experiments are shown in Fig. 4 for the case where both crystallographically equivalent ligand positions are occupied by the same ligand (e.g., bpy, bprid or bpy-d_8, etc.). When the luminescence is observed at the red edge of the inhomogeneous distribution, an intensity ratio of $\approx$1:1 is expected for the narrowed line to the broad feature.

In Fig. 5 we show excitation line narrowing experiments for the origin III in the series $[Ru(bpy)_{3-x}(bprid)_x]^{2+}$ (x = 1 to 3). Red edge luminescence in the origin I has been observed with a narrow bandwidth in these experiments. Origin III in the x = 1 system shows a single narrowed line and no broad feature. This is because the ^{3}MLCT origins involving the transitions to the bpy ligand in the crystallographically equivalent position are thousands of wavenumbers higher in energy.

The x = 2 and x = 3 systems show a narrowed feature and a broad feature with intensity ratios of $\approx$2:1 and $\approx$1:1, respectively. These ratios simply relate to the occupancy by a bprid ligand of the crystallographically equivalent ligand position. The narrowing

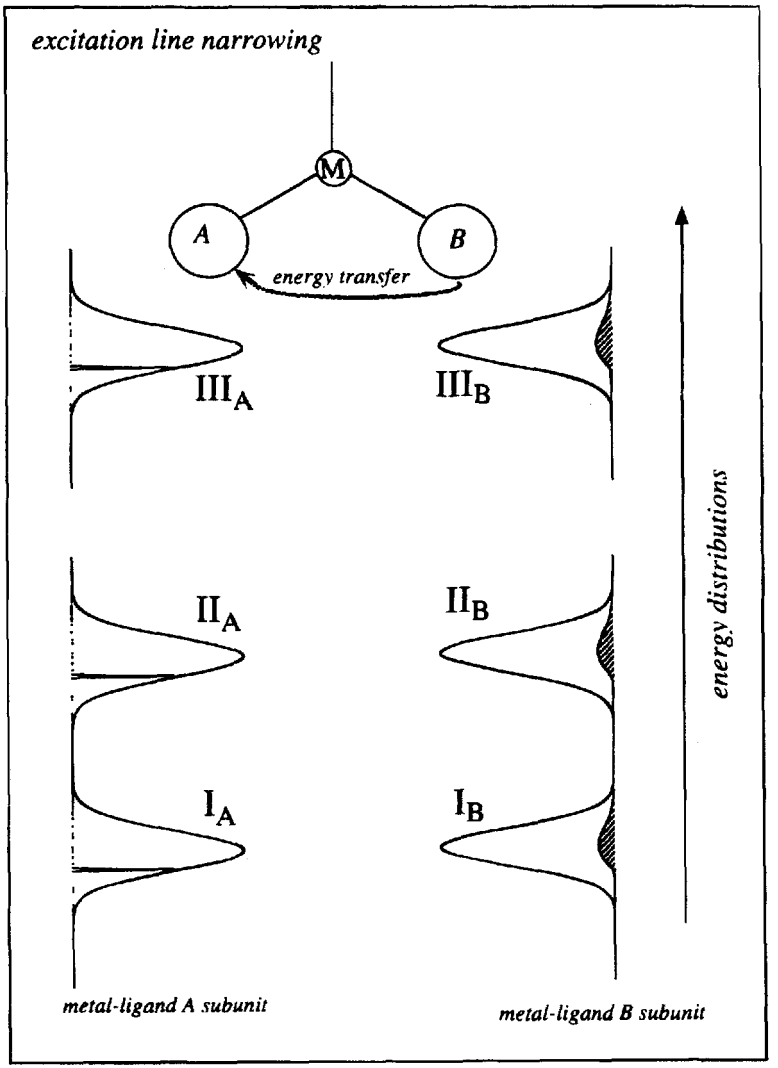

FIGURE 3 Schematic representation of excitation line narrowing experiments for localised ^{3}MLCT transitions in a system with two crystallographically and chemically equivalent ligands (i.e., A = B = bpy, bpy-d_8, bprid, etc.). The transitions involving the ligand A are narrowed by selectively monitoring the origin I. Independent distributions for the ^{3}MLCT energies involving A or B are assumed. The shaded area highlights the distribution of metal-ligand B subunits which are deactivated by excitation energy transfer to the metal-ligand A subunit.

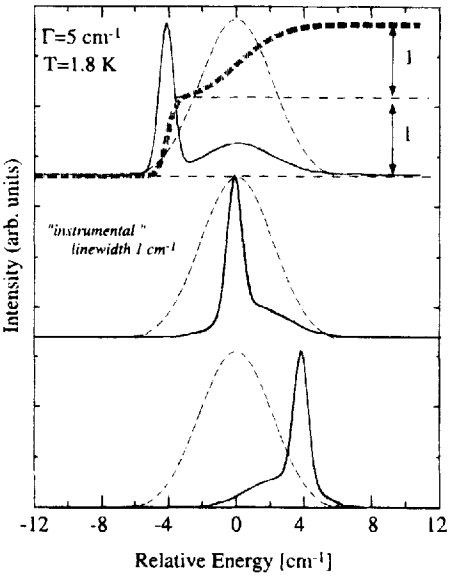

FIGURE 4 Simulated excitation line narrowing spectra of localised ^{3}MLCT transitions for three "observation" wavelengths (red edge, center and blue edge from top to bottom) in a system with two crystallographically and chemically equivalent ligands. The inhomogeneous distribution and the integral of one of the spectra are indicated by dashed lines.

experiments establish[24] that the lowest-energy ^{3}MLCT transitions are localised and the excitation exchange interaction β between Rubprid subunits is less than 0.5 cm^{-1}.

4. LOCALISED ^{3}MLCT STATES IN RUTHENIUM COMPLEXES

4.1 Deuteration Effects

If one takes an excitation which is delocalised over the entire molecule such as π-π^* transitions, a gradual shift of the energy of the origins as a function of the deuteration degree is observed.[17] For example, benzene, naphthalene and anthracene show a nearly linear shift of +33 cm^{-1}, 15 cm^{-1} and 6 cm^{-1}, respectively, per substituted

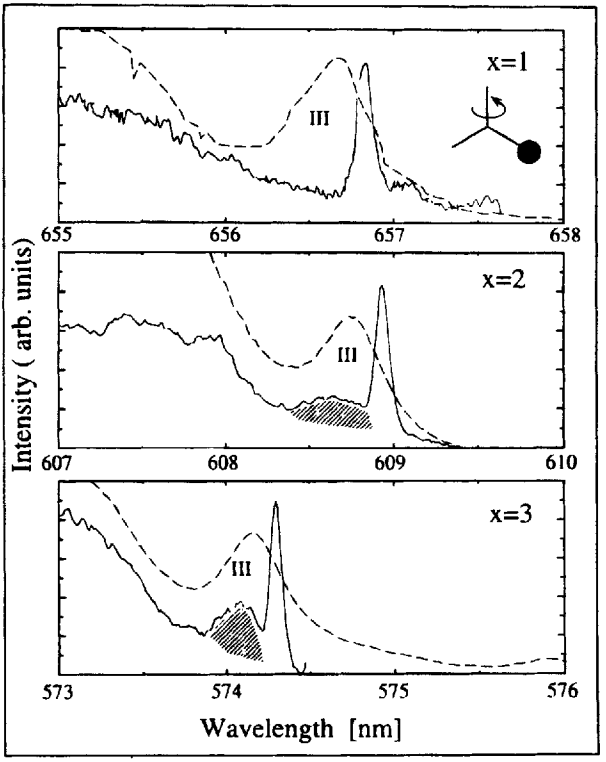

FIGURE 5 Excitation line narrowing of origin III in the series $[Ru(bpy)_{3-x}(bprid)_x]^{2+}$ (x = 1 to 3) in $[Zn(bpy)_3](ClO_4)_2$ at liquid helium temperatures (Ref. 24).

hydrogen. The spectroscopy of the electronic origins of the series $[M(bpy)_{3-x}(bpy\text{-}d_8)_x]^{2+}$ (x = 0 to 3; M = Ru, Os) provides a direct answer to the localisation/delocalisation question. A gradual shift of the origins to higher energy would result if the lowest-excited ^{3}MLCT were true molecular states of all three ligands. Gradual shifts would also result if these states were excitons with a value of β at least of the same order of magnitude as the deuteration shift.

In Fig. 6 excitation and luminescence spectra are shown in the region of the lowest-energy electronic origins for the $[Ru(bpy)_{3-x}(bpy\text{-}d_8)_x]^{2+}$ (x = 0 to 3) series in the $[Zn(bpy)_3](ClO_4)_2$ lattice.[28] A doubling of the electronic origins I, II and III is observed in excitation

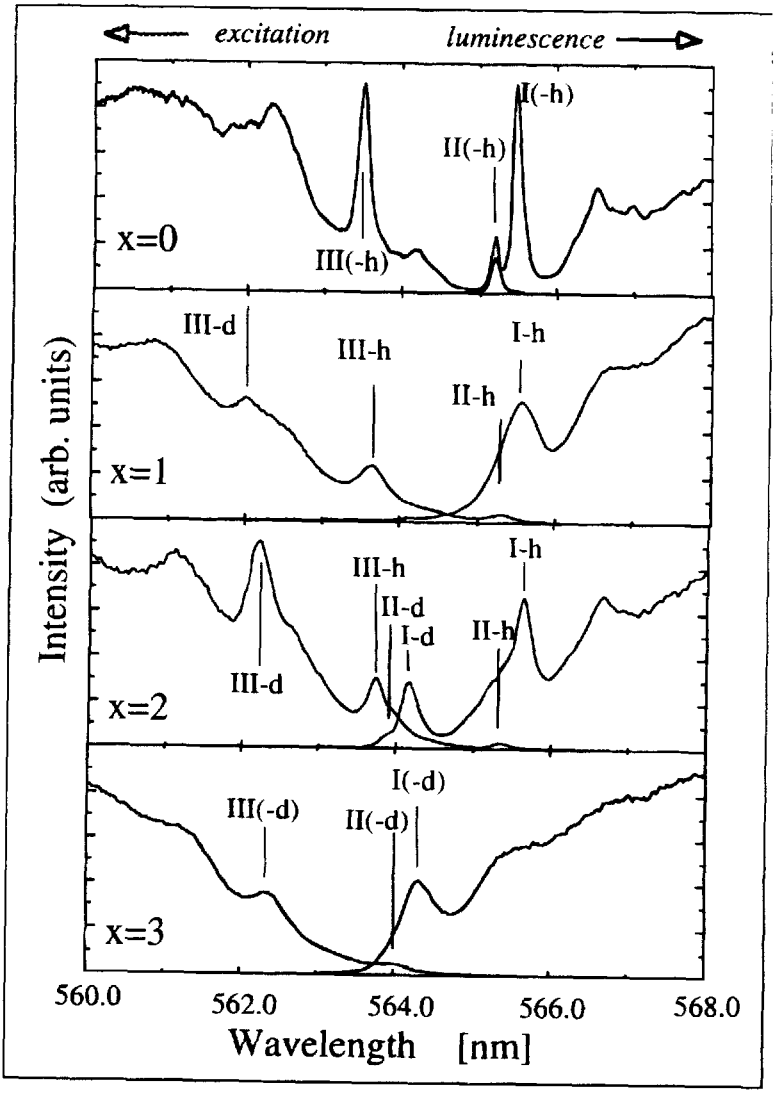

FIGURE 6 Non-selective excitation and luminescence spectra of the series $[Ru(bpy)_{3-x}(bpy\text{-}d_8)_x]^{2+}$ (x = 0 to 3) in $[Zn(bpy)_3](ClO_4)_2$ at 1.8 K. Transitions involving the protonated and the deuterated ligands are denoted by -h and -d, respectively (Ref. 28).

for the x = 1 and x = 2 systems and in luminescence for the x = 2 system. The two sets of origins are very close in energy to the origins observed for the perprotonated (x = 0) and perdeuterated (x = 3) complexes and are associated with independent transitions involving the bpy-h_8 or the bpy-d_8 ligand. (The two sets are labelled as -h and -d, respectively, in Fig. 6). The excitation exchange interaction is much smaller than the deuteration shift and also less than the inhomogeneous broadening of the electronic origins. In the x = 2 system, luminescence involving the bpy-d_8 ligand (origins I-d, II-d) occurs because both crystallographically equivalent ligands can be substituted by bpy-d_8 (see Fig. 1). We stress again that ^{3}MLCT transitions involving the bpy-h_8 ligand in the distinct ligand position are several hundred wavenumbers higher in energy. In the x = 1 system, fast intramolecular excitation energy transfer ensures that luminescence involves only a bpy-h_8 ligand.

In contrast, a linear shift (and no doubling) of the origins is observed in the systems $[Ru(bpy\text{-}d_x)_3]^{2+}$ (x = 0, 2, 6, 8) as is illustrated in Fig. 7.

Braun et al.[29] have interpreted the spectra of partially deuterated complexes $[Ru(bpy)_{3-x}(bpy\text{-}d_8)_x]^{2+}$ (x = 1,2) in terms of two crystallographic sites. Their hypothesis can be refuted on the basis of the observed intensity ratios in absorption and non-selective and narrowed excitation and luminescence.[28] Similarly, the $[Os(bpy)_{3-x}(bpy\text{-}d_8)_x]^{2+}$ series was interpreted[30] using a variable number of sites. The spectroscopy of this latter series can also be understood on the basis of the one site C2/c crystal structure (see Section 5.2 and Ref. 23).

Support for our description also stems from the following points:

- observed origins (I, II, III)-h and (I, II, III)-d in the x = 1 and x = 2 systems coincide with the origins of the x = 0 and x = 3 systems;
- intensity ratios between narrowed and broad features observed in excitation and luminescence line narrowing experiments[24,31];
- variation of the coupling of vibrational sidelines (see Section 6)[24];
- longer lifetime observed for the "deuterated" emission in comparison with the "protonated" emission[28];

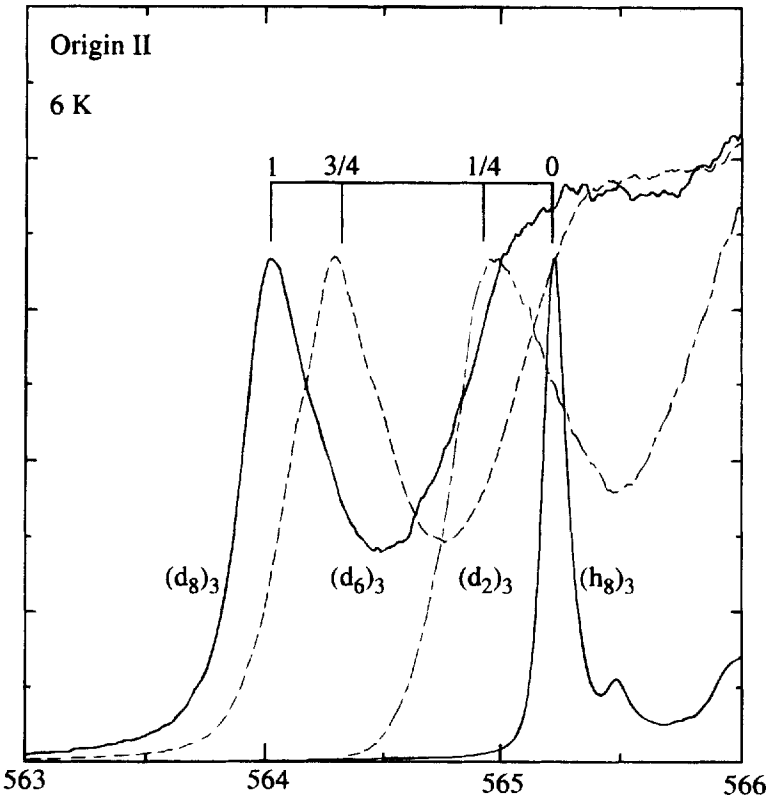

FIGURE 7 Luminescence spectra at 6 K of $[Ru(bpy\text{-}3,3'\text{-}d_2)_3]^{2+}$ and $[Ru(bpy\text{-}4,4',5,5',6,6'\text{-}d_6)_3]^{2+}$ in $[Zn(bpy)_3](ClO_4)_2$ in comparison with the spectra of the perprotonated and perdeuterated complex (Ref. 33).

- spectroscopy of the bprid/bpy and bpy/phen series (see Sections 3 and 5.3);
- observed temperature dependence of the "deuterated" luminescence in the x = 2 and x = 1 complex.[32]

Clear confirmation for our assignments of the origins in the $[Ru(bpy)(bpy\text{-}d_8)_2]^{2+}/[Zn(bpy)_3](ClO_4)_2$ system is found in the emission

of the $[Ru(bpy)(bpy\text{-}d_6)_2]^{2+}$ and $[Ru(bpy\text{-}d_2)(bpy\text{-}d_8)_2]^{2+}$ complexes in $[Zn(bpy)_3](ClO_4)_2$ shown in Fig. 8. The origins involving the bpy-d_6 or the bpy-d_2 ligands shift to lower or higher energy, respectively, in comparison with the transitions involving the bpy-d_8 or the bpy-h_8 ligand in the $[Ru(bpy)(bpy\text{-}d_8)_2]^{2+}$ system, and they coincide with the origins of $[Ru(bpy\text{-}d_6)_3]^{2+}$ and $[Ru(bpy\text{-}d_2)_3]^{2+}$ (Fig. 7). In contrast, the origins of the bpy-h_8 and bpy-d_8 ligands in the $[Ru(bpy)(bpy\text{-}d_6)_2]^{2+}$ and $[Ru(bpy\text{-}d_2)(bpy\text{-}d_8)_2]^{2+}$ complexes coincide with the corresponding origins in $[Ru(bpy)(bpy\text{-}d_8)_2]^{2+}$.[33]

Luminescence spectra of the series $[Ru(bpy)_{3-x}(bpy\text{-}d_8)_x](PF_6)_2$ are shown in Fig. 9. Luminescence in these neat systems is dominated by the lowest-energy site because *intermolecular* energy transfer is much faster than the lifetime of the lowest-excited ^{3}MLCT states.

The spectra shown in Fig. 9 demonstrate the localised nature of the lowest-excited states. Emission occurs only from the bpy-h_8 ligand in the x = 1 and x = 2 system,[34] as *intramolecular* energy transfer between the three crystallographically equivalent ligands is fast.

Again, a gradual shift is observed[32] when all three ligands have the same deuteration degree. For example, the observed shift for $[Ru(bpy\text{-}3,3'\text{-}d_2)_3](PF_6)_2$ is about a fourth of the full deuteration shift, as one fourth of the protons have been substituted by deuterons.

4.2. Excitation and Luminescence Line Narrowing Experiments

Excitation line narrowing experiments[31,24] in origin III of the series $[Ru(bpy)_{3-x}(bpy\text{-}d_8)_x]^{2+}$ (x = 0 to 3) in $[Zn(bpy)_3](ClO_4)_2$ are summarized in Fig. 10. As in the bprid/bpy series (Section 3) these experiments are crucial in demonstrating the independence of the ^{3}MLCT transitions involving either of the two crystallographically equivalent ligands.

The intensity ratios between narrowed and broad features simply reflect the occupancy of the crystallographically equivalent ligand position by a like ligand, i.e., bpy or bpy-d_8. No broad feature can be detected in excitation line narrowing experiments of origin III-h in the x = 2 system, as the crystallographically equivalent ligand position is occupied by bpy-d_8 whose corresponding transition (III-d) is $\approx$40 cm^{-1} higher in energy. In contrast the ratio is about 1:1

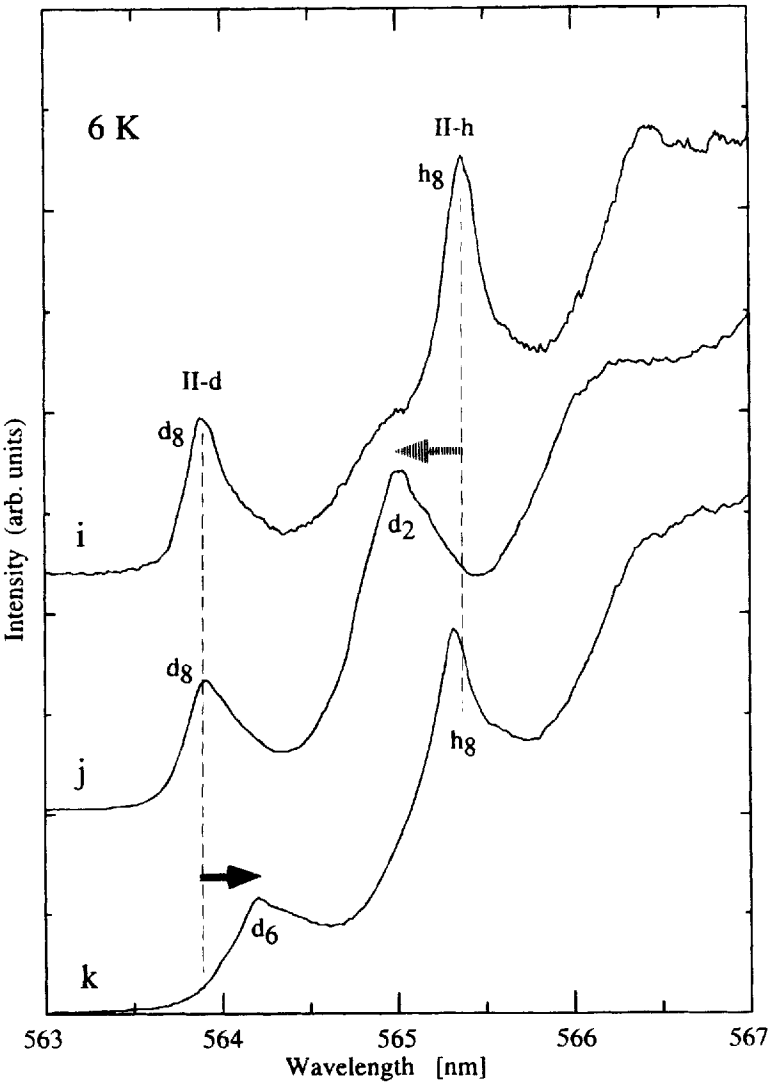

FIGURE 8 Luminescence spectra at 6 K of (j) $[Ru(bpy\text{-}3,3'\text{-}d_2)(bpy\text{-}d_8)_2]^{2+}$ and (k) $[Ru(bpy)(bpy\text{-}4,4',\ 5,5',\ 6,6'\text{-}d_6)_2]^{2+}$ in $[Zn(bpy)_3](ClO_4)_2$ in comparison with the spectrum of (i) $[Ru(bpy)(bpy\text{-}d_8)_2]^{2+}$ (Ref. 33).

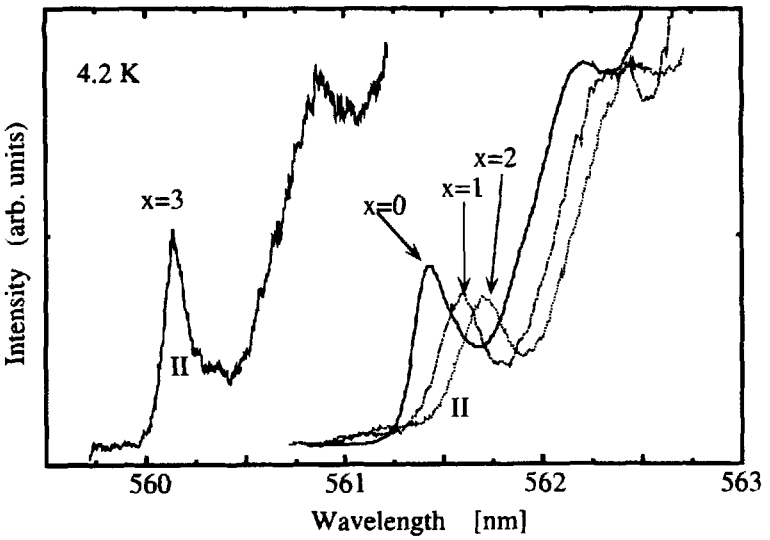

FIGURE 9 Luminescence spectra of the series $[Ru(bpy)_{3-x}(bpy\text{-}d_8)_x](PF_6)_2$ (x = 0 to 3) at 4.2 K (Ref. 34).

when the emission is monitored at the red edge of origin I-d in the x = 2 system because "deuterated" emission occurs only when both crystallographically equivalent ligands are substituted by bpy-d_8.

Complementary results were obtained in luminescence line narrowing experiments.[28] In particular, the I-h/II-h origins of the x = 2 systems show only narrowed features independent of the wavelength of excitation within origin III-h. This is because there is only one bpy-h_8 ligand. The I-d/II-d origins show broad features which are very pronounced when the wavelength of excitation is at the blue edge of origin III-d. The broad features are again due to the bpy-d_8 ligand in the crystallographically equivalent position.

4.3. Time Resolved Luminescence Line Narrowing

As both crystallographically equivalent ligands can be observed in line narrowing experiments, it is possible to directly measure excitation energy transfer between the two subunits by means of time resolved luminescence line narrowing experiments.[31]

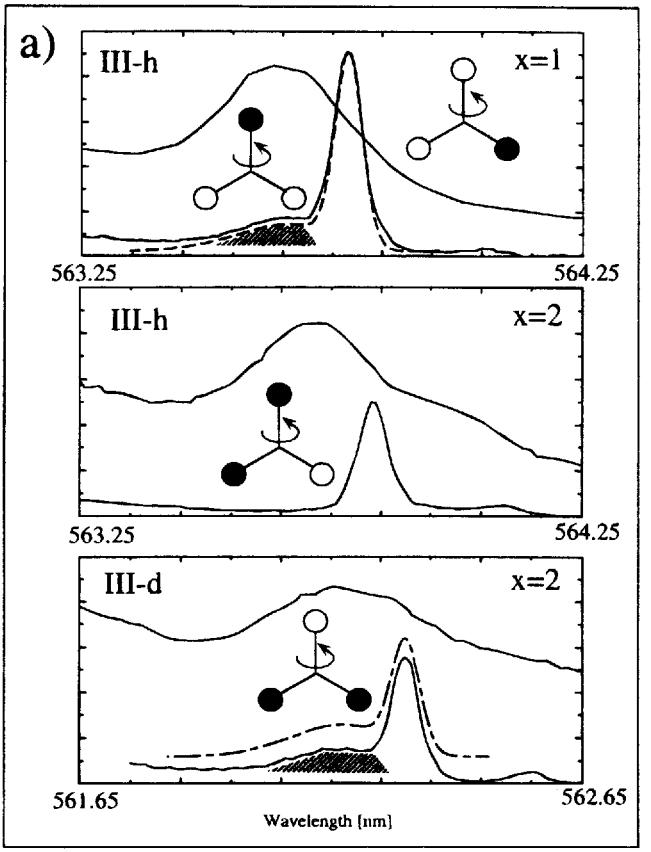

FIGURE 10 Excitation line narrowing of the origin III in the series $[Ru(bpy)_{3-x}(bpy\text{-}d_8)_x]^{2+}$ (x = 0 to 3) in $[Zn(bpy)_3](ClO_4)_2$ at 1.8 K. The luminescence was monitored at the red edge of the origin I for all spectra. The shading indicates the broad feature due to the like ligand in the crystallographically equivalent position (Refs. 24 and 31).

After pulsed excitation, origin II is observed as a transient because the II $\rightarrow$ I intra metal-ligand subunit relaxation is relatively slow ($k \approx 5 \times 10^6\ s^{-1}$).[35] Excitation energy transfer (between the equivalent metal-ligand subunits) in level II can then be observed. In Fig. 11 results[31] are shown for the II-d origin of the $[Ru(bpy)(bpy\text{-}d_8)_2]^{2+}$ complex doped in $[Zn(bpy)_3](ClO_4)_2$. The luminescence was excited

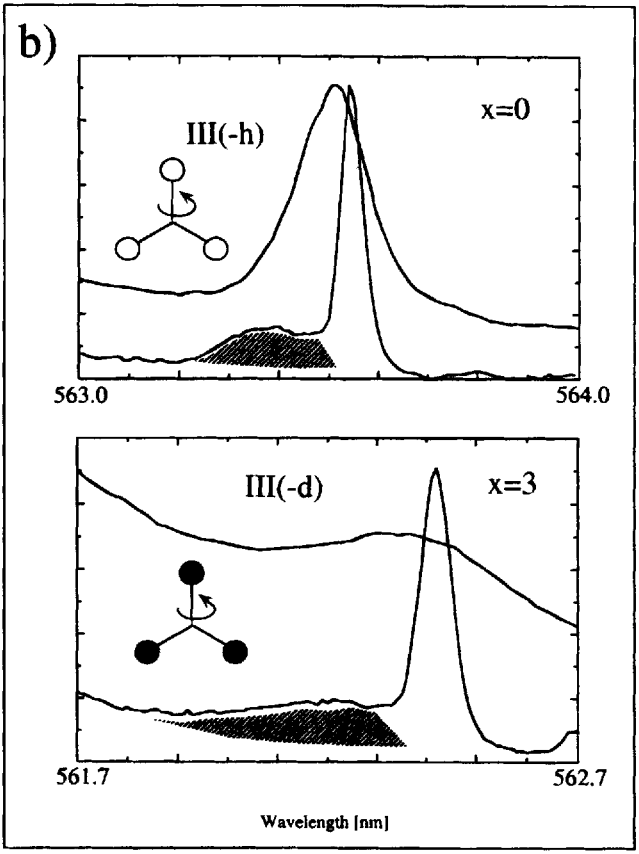

FIGURE 10 *Continued*

at the blue edge of origin III-d. The broad feature is due to the second ligand which is activated by excitation energy transfer from the metal-ligand subunit whose II-d transition is narrowed.

The narrowed feature shows a fast decay in the first 20 ns because excitation energy (i.e., the electron) is transferred to the bpy-d_8 ligand in the crystallographically equivalent position if its energy is lower. The broad feature shows a corresponding rise. Both decay curves then approach the II $\rightarrow$ I relaxation rate.

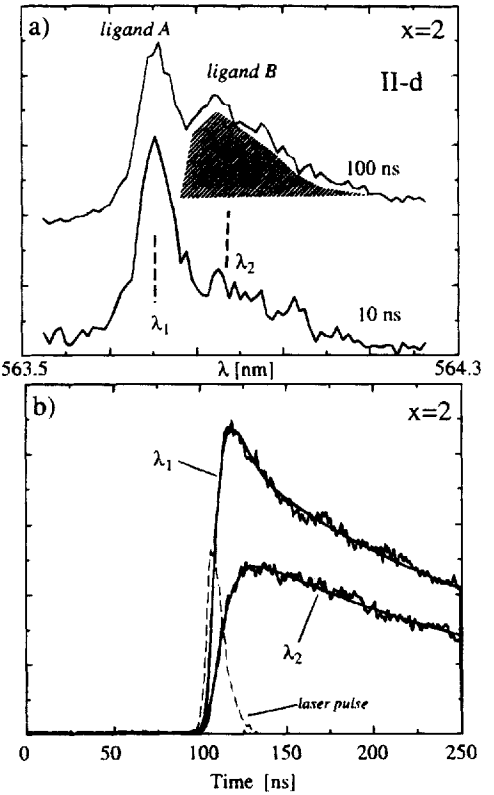

FIGURE 11 Time resolved luminescence line narrowing experiments in the II-d origin of $[Ru(bpy)(bpy\text{-}d_8)_2]^{2+}$ in $[Zn(bpy)_3](ClO_4)_2$ at nominal 1.8 K. In (a) the luminescence was monitored for the first 10 ns or the first 100 ns after the laser pulse rise. In (b) the decay curves measured at the indicated wavelengths λ_1 and λ_2 are shown (Ref. 31).

A critical, internal "blank" experiment is provided by the II-h emission (not illustrated here) which shows a single narrowed feature because there is only one bpy-h_8 ligand in the x = 2 system. The decay waveform is purely given by the shape of the laser pulse and the II $\rightarrow$ I relaxation rate in this case. A sum of the transfer and back transfer rate, $k_{et} + k_{bt}$, of 1.3×10^8 s^{-1} has been obtained at 1.8 K for *intramolecular* energy transfer in level II. The same rate

has been deduced for the perprotonated and perdeuterated complex in the same host.[31]

The excitation energy transfer from deuterated to protonated metal-ligand subunits is even faster.[32] The energy gap between the two systems is ≈ 37 cm^{-1}, and thus the much larger density of phonon states enables fast energy transfer. Also, the origins II-d and III-h partially overlap, enabling resonant transfer.

4.4. Stark Experiments

It is informative to apply electric fields (Stark experiments) to MLCT transitions. An electric field was applied[36] perpendicular to the crystal *b* and *c* axes (see Fig. 12) for $[Ru(bpy)_3]^{2+}$ in $[Zn(bpy)_3](ClO_4)_2$. The two crystallographically equivalent ligands become inequivalent as the MLCT transitions to ligands A and B shift to lower and higher energy, respectively. Thus a pseudo-Stark splitting of origins results. Intramolecular excitation energy transfer thermalises the levels within the lifetime of the luminescence.

The pseudo-Stark splitting of the three lowest-energy origins can be determined from luminescence and excitation spectra. The splittings are the same for all three origins.[36] In Fig. 13 the splitting of origin III is illustrated in non-selective and narrowed excitation spectra measured at 1.8 K. The splitting of origin I is determined from the luminescence spectrum taken at the same temperature (insert of Fig. 13). The large effect (1.2 eÅ) establishes directly the charge-transfer character of the three lowest-excited states.

The narrowed excitation spectra again show that the transitions to ligands A and B are poorly correlated. When the origin I-A (= lowest-energy ^{3}MLCT origin involving the ligand A) is observed in emission with a narrow bandwidth, the origin III-A is narrowed, but the energy of III-B is spread almost over the entire inhomogeneous distribution.[36]

4.5. High Resolution Narrowing Experiments

The large Stark effect observed for the origins I, II and III made Stark-swept transient hole-burning experiments feasible.[37] We feel this to be one of the most elegant optical experiments ever performed on a coordination compound. An upper limit for the homogeneous

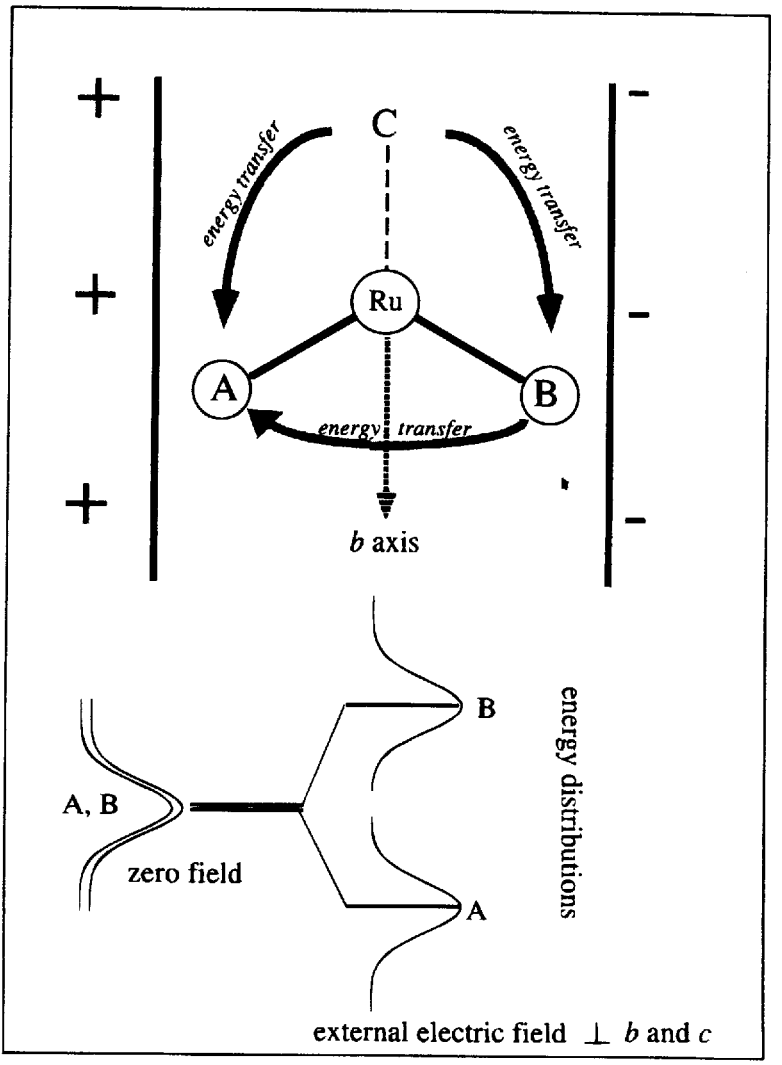

FIGURE 12 Schematic representation of the Stark experiments performed on $[Ru(bpy)_3]^{2+}$ in $[Zn(bpy)_3](ClO_4)_2$ (Ref. 36).

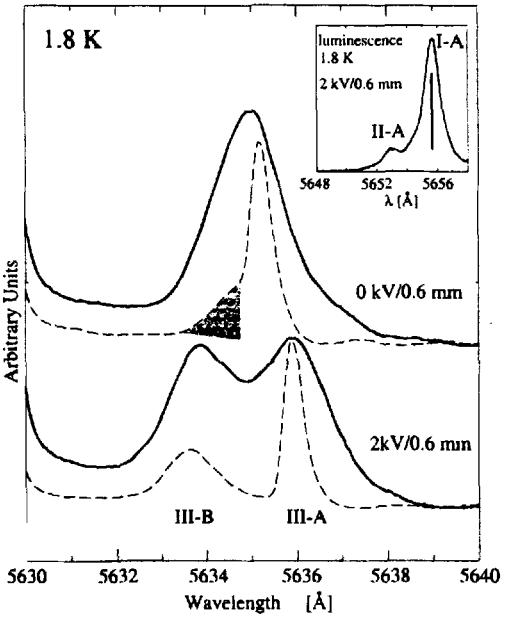

FIGURE 13 Pseudo-Stark splitting of origin III of $[Ru(bpy)_3]^{2+}$ in $[Zn(bpy)_3](ClO_4)_2$ as observed in non-selective (solid line) and narrowed (dashed line) excitation spectra at 1.8 K (Ref. 36).

linewidth of ≈15 MHz (= 0.0005 cm^{-1}) has been deduced for origin II at 1.5 K.

The rate of direct relaxation to level I is about 5×10^6 s^{-1} and thus cannot be responsible for the observed width. It then follows that the intramolecular excitation energy transfer cannot be faster than ≈10 ns, at least for the chromophores responsible for the hole. This value is in agreement with the directly measured rate (Section 4.3).

We have also performed high resolution luminescence line narrowing experiments. An upper limit of about ≈25 MHz has been deconvoluted for origin II at 4.2 K. These experiments establish that the energy correlation within the inhomogeneous distribution of origins I and II on a single metal-ligand subunit is better than 2%.[37]

4.6. Zeeman Effects

We have reported a detailed study of the Zeeman effect of the lowest-excited ^{3}MLCT levels in the $[Ru(bpy)_3]^{2+}$ complex doped in the $[Zn(bpy)_3](ClO_4)_2$ host.[36,38] The observed dependence of line positions, line shapes and intensities on the angle between the magnetic field and the crystal *b* axis in the metal-ligand plane is quantitatively accounted for with one single set of parameters (effective g-values) in simulations which are based on treating the Zeeman effect individually for each ligand, i.e., a localised model.[36,38]

The Zeeman effects in $[Ru(bpy)_3](PF_6)_2$ observed for the origins I and II can also be quantitatively accounted for by using a localised description.[38] The effective g-values for the three metal-ligand subunits are found to be the same as for the two crystallographically equivalent subunits in the $[Zn(bpy)_3](ClO_4)_2$ host. No splittings of the origins I and II are observed[39] in fields B‖c, and the magnetic circularly polarised luminescence is due to $\mathcal{B}$ terms.[40] These results indicate that the three lowest-excited levels (I, II and III) on one metal-ligand subunit are the components of an orbitally non-degenerate spin triplet.

4.7. A Mixed Ligand System

The spectroscopy of $[Ru(bpy)_{3-x}(phen)_x]^{2+}$ (x = 0 to 3) series in $[Zn(bpy)_3](ClO_4)_2$ is useful because the ^{3}MLCT states are close lying and thus complement the work on deuterated systems.[41] Figure 14 shows excitation and luminescence spectra in the region of the electronic origins of the x = 1 system. Two sets of origins can be observed in the luminescence and excitation spectra. Their energy spacings are characteristic, and it is straightforward to assign the sets at higher and lower energy to the ^{3}MLCT transitions involving the bpy and the phen ligand(s), respectively.

In the narrowed excitation spectrum of the transitions involving the phen ligand, a doubling is observed because the I-phen/II-phen energy separation is less than the inhomogeneous broadening, i.e., both I-phen and II-phen are monitored in the line narrowing experiments.

The lowest-energy ^{3}MLCT origin involving the phen ligand is $\approx 125\ cm^{-1}$ lower in energy than the corresponding transition involving the bpy ligand. The luminescence of the x = 1 system consists of two overlapping spectra. ^{3}MLCT emission involving the phen or the bpy ligand occurs when one of the crystallographically equivalent

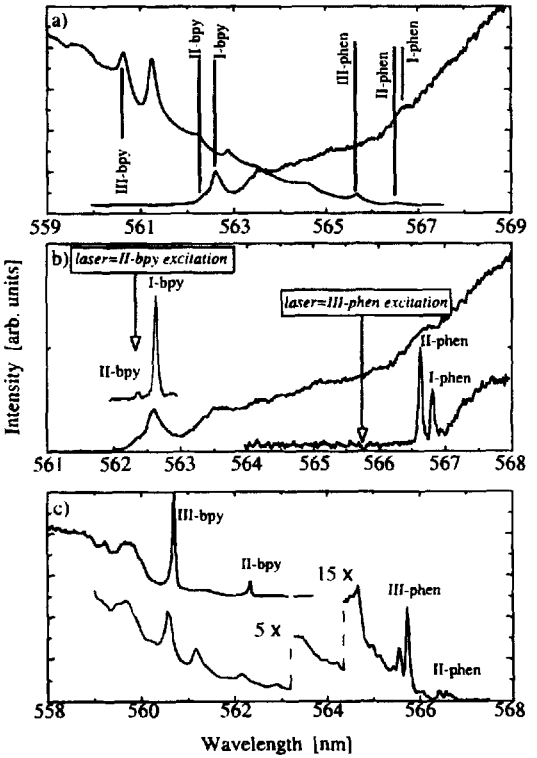

FIGURE 14 Luminescence and excitation spectra of $[Ru(bpy)_2(phen)]^{2+}$ in $[Zn(bpy)_3](ClO_4)_2$ at 1.8 K. (Ref. 41). (a) Non-selective excitation and luminescence spectra. (b) Narrowed luminescence spectra for bpy and phen in comparison with the non-selectively excited luminescence. (c) Narrowed excitation spectra for the bpy and phen transitions.

bpy ligands or the distinct ligand of the host is substituted by the phen ligand, respectively. In the latter case emission from the bpy ligand occurs because the phen ligand in the distinct position again lies several hundred wavenumbers higher in energy. Excitation involving this ligand is then deactivated by intramolecular energy transfer. Intramolecular excitation energy transfer also ensures that in the x = 2 system only emission involving the phen ligand is observed.

We stress that the relative intensities and energies of the origins remain almost constant for the bpy and the phen ligands within the

series.[41] This establishes that the excitation exchange interaction β between metal-ligand subunits is smaller than 0.5 cm^{-1}.

5. INTRAMOLECULAR ^{3}MLCT EXCITONS

The $[Os(bpy)_3]^{2+}$ complex in crystalline environments is particularly interesting, as the lowest-excited states are best described as coherent intramolecular excitons with weak excitation exchange interactions β (see Introduction). The magnitude and sign of β is dependent on the host and is substantially larger than the value for ruthenium systems.

5.1 $[Os(bpy)_3]^{2+}$ in $[Ru(bpy)_3](PF_6)_2$

Emission of the $[Os(bpy)_3]^{2+}$ complex occurs from the three crystallographic sites (labelled $\mathcal{A}$, $\mathcal{B}$, and $\mathcal{C}$ from lower to higher energy) provided by the host.[42] Intermolecular energy transfer between the osmium complexes is not efficient at low concentration of the dopant.

The excitation exchange interaction β is -2.3 cm^{-1} in $[Os(bpy)_3]^{2+}$ doped into this trigonal host.[43] This small value leads to some spectacular effects in the spectroscopy of the lowest-excited states in the series $[Os(bpy)_{3-x}(bpy\text{-}d_8)_x]^{2+}$ (x = 0 to 3), as the deuteration shift ($\approx$32 cm^{-1}) is substantially larger than β. In the x = 1 system the lowest-energy exciton resides on the two bpy-h_8 ligands, whereas in the x = 2 system full localisation on the single bpy-h_8 ligand occurs. Figure 15 shows excitation and luminescence spectra of origin I of the lowest-energy site $\mathcal{A}$ for the series $[Os(bpy)_{3-x}(bpy\text{-}d_8)_x]^{2+}$ (x = 0 to 3) in $[Ru(bpy)_3](PF_6)_2$.

The x = 0 and x = 3 systems show a 7 cm^{-1} splitting of origin I. The lower component is very weak and can be assigned to the forbidden A level whose wavefunction is given in Eq. (3). This ordering of the levels (A lower than E) determines the sign of β.

In the x = 1 system the splitting is 5 cm^{-1} which is in quantitative agreement with a calculation based on Eq. (2) using $\beta = -2.3$ cm^{-1} and a deuteration shift Δ = 32 cm^{-1} for one ligand. The theoretical intensity ratio is $\approx$3:1 (lower to higher component) and in reasonable agreement with the observed ratio of $\approx$2:1. Origin I shows a single transition in excitation and luminescence in the x = 2 system, as there is only one bpy-h_8 ligand.

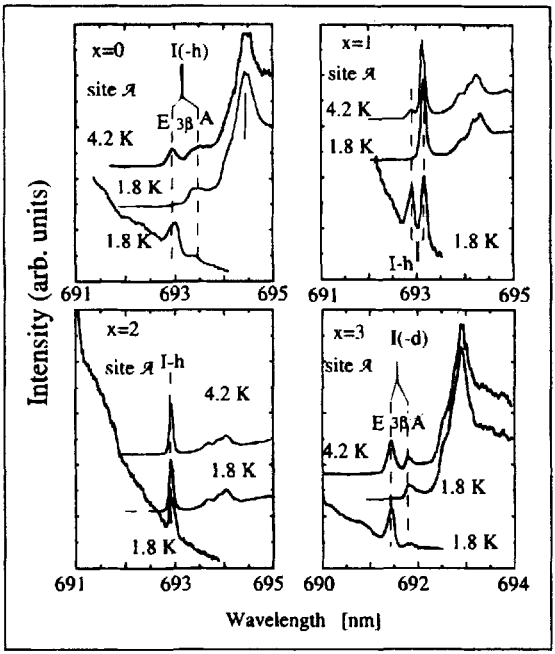

FIGURE 15 Excitation and luminescence spectra in the region of the lowest-energy electronic origins of site $\mathcal{A}$ of $[Os(bpy)_{3-x}(bpy\text{-}d_8)_x]^{2+}$ (x = 0 to 3) in $[Ru(bpy)_3](PF_6)_2$ at liquid helium temperatures. The exciton splitting is indicated for the x = 0, 1 and 3 systems (Ref. 43).

Excitation spectra of the series in the region of origin II are shown in Fig. 16 for the highest-energy site $\mathcal{C}$. The x = 1 and x = 2 systems show independent transitions to the bpy-h_8 ligand(s) (II-h) and the bpy-d_8 ligand(s) (II-d). The intensity ratio is ≈2:1 and ≈1:2 for the x = 1 and x = 2 systems, reflecting the number of protonated and deuterated ligands. Origin II-h in the x = 1 system shows an exciton splitting of ≈4 cm^{-1} in the x = 1 system, whereas this origin consists of one single line which can be considerably narrowed in the x = 2 system. Origin II-d consists of one single line in the x = 1 system but shows some unresolved splitting in the x = 2 system.

Significant narrowing of origins I-h and II-h is seen in luminescence and excitation for the x = 2 system. Again, energies are well correlated on a single metal-ligand subunit. Nanoheterogeneity in

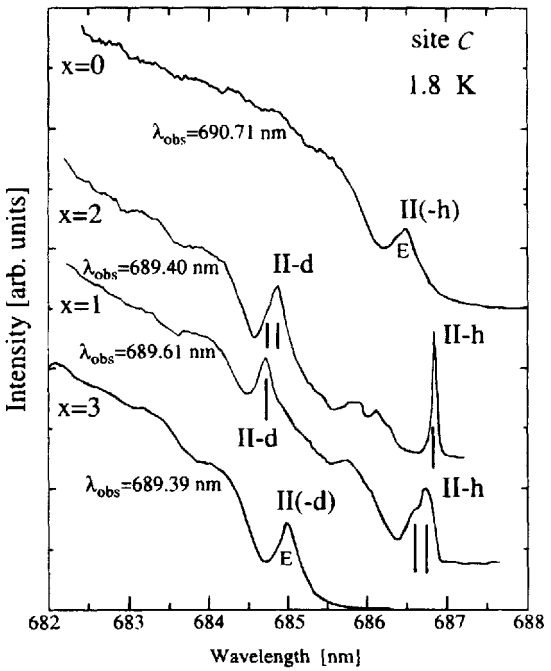

FIGURE 16 Excitation spectra of site C of $[Os(bpy)_{3-x}(bpy\text{-}d_8)_x]^{2+}$ (x = 0 to 3) in $[Ru(bpy)_3](PF_6)_2$ in the region of the second origin II. Exciton splittings are indicated for II-h (x = 1) and II-d (x = 2) (Ref. 43).

this lattice is comparable to β. An important consequence of this is that spectral features associated with two or three coupled ligands cannot be substantially narrowed. This can be used as a "fingerprint" for weakly coupled excitons where the excitation exchange interaction is of the same order of magnitude as the nanoheterogeneity.[43]

One can envisage a "quantum beat" experiment in which a resonant fs-ps pulse is used to create a coherent excitation of the system. Oscillations or "beats" would be observed at a frequency of ≈22 GHz corresponding to the excitation exchange interaction.[16]

5.2. $[Os(bpy)_3]^{2+}$ in $[M(bpy)_3](ClO_4)_2$ (M = Ru, Zn)

The spectroscopy of the series can be understood[23,44] in terms of the C2/c crystal structure (which has one site for the cation) and

with MLCT transitions to the distinct ligand being higher in energy. $[Os(bpy)_{3-x}(bpy\text{-}d_8)_x]^{2+}$ with x = 1 and x = 2 can enter the $[Zn(bpy)_3](ClO_4)_2$ host in the two ways shown in Fig. 1.

In Fig. 17 the luminescence spectra of the series are shown in the region of the electronic origins at 1.8 K. The same pattern shifted to the red by ≈56 cm^{-1} is observed for the isomorphous $[Ru(bpy)_3](ClO_4)_2$ host.[23] The x = 1 and x = 2 systems show two

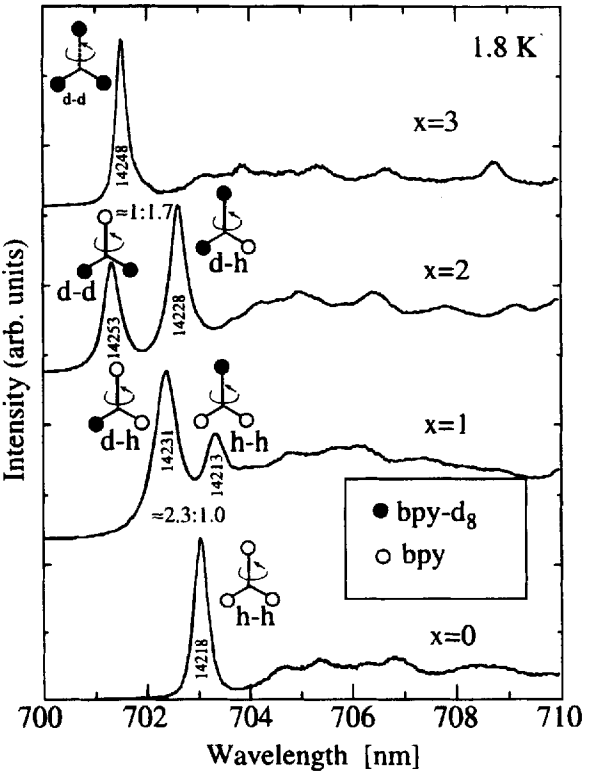

FIGURE 17 Luminescence spectra in the region of the electronic origins of the series $[Os(bpy)_{3-x}(bpy - d_8)_x]^{2+}$ (x = 0 to 3) in $[Zn(bpy)_3](ClO_4)_2$ at 1.8 K. The x = 1 and x = 2 complexes can substitute in two ways into the C2/c lattice (see Fig. 1). The origins are assigned to these two substitutions. Energies of the origins are indicated (Ref. 44).

electronic origins in luminescence, whereas the x = 0 and x = 3 systems have one origin.

These origins can be assigned to the complexes which enter the lattice by substituting the crystallographically equivalent ligands both by bpy, or one bpy and one bpy-d_8 or both by bpy-d_8. We abbreviate these species as h-h, d-h and d-d, respectively. In contrast to the PF_6 lattice discussed in the previous section, β is at least of the same order of magnitude as the deuteration shift. This follows from the observation that the d-h species has its lowest-energy origin about halfway between the x = 0 and x = 3 systems and that the observed intensity ratios of ≈1:2.3 for h-h:d-h and ≈1:1.7 for d-d:d-h in the x = 1 and x = 2 systems, respectively, reflect the probabilities of h-h, d-h, and d-d substitutions in the lattice. Deviations from ideal ratios arise from changes in the quantum efficiency and the exciton splitting.

We have investigated the series $[Os(bpy)_{3-x}(bpy\text{-}d_8)_x]^{2+}$ (x = 0 to 3) doped in $[Zn(bpy)_3](ClO_4)_2$ and in $[Ru(bpy)_3](ClO_4)_2$ by selective excitation spectroscopy. Four electronic origins can be identified in the region of the lowest-energy excitations.[23,44] They can be accounted for in terms of the excitonic formalism outlined in the Introduction. The excitation exchange interaction β between the two crystallographically equivalent ligands is β ≈ 79 cm^{-1} and β ≈ 77 cm^{-1} in level II in the $[Zn(bpy)_3](ClO_4)_2$ and $[Ru(bpy)_3](ClO_4)_2$ hosts, respectively. The excitation coupling is smaller in level I with β ≈ 37.5 cm^{-1} in both hosts.[23,44]

A test of these assignments can be made by inserting the deuteration shift of 32 cm^{-1} and the coupling constants β into Eq. (5) to describe the d-h species of the x = 1 and x = 2 systems. Observed and calculated energy levels are summarised in Fig. 18. Overall agreement is most satisfactory.

6. VIBRATIONAL SIDELINES

All electronic excitations, whether metal centered, ligand centered or charge transfer, involve some rearrangement of charge. Vibrational sidelines can be coupled to the electronic excitation. The extent to which any particular mode is coupled is of course specifically related to the nuclear displacements between the ground and an excited

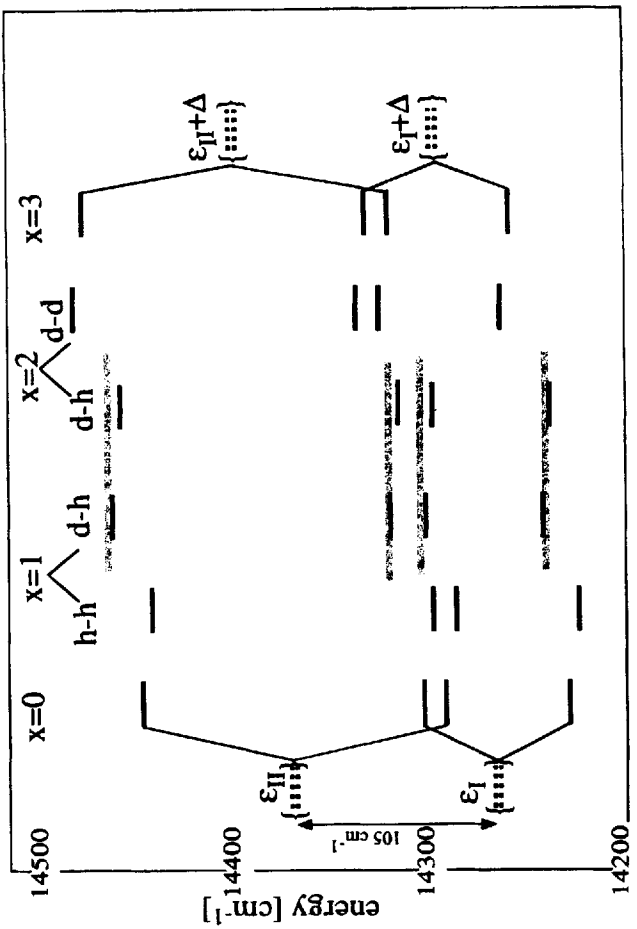

FIGURE 18 Summary of observed (Ref. 23) electronic levels in the series $[Os(byp)_{3-x}(bpy\text{-}d_8)_x]^{2+}$ in $[Zn(byp)_3](ClO_4)_2$. The dotted lines indicate the extrapolated energies ϵ_i (= barcicenters of two Davidov components). The shaded bars indicate calculated energies for the x = 1 and x = 2 systems. These calculations are based on the data obtained for x = 0 and x = 3 systems.

electronic state. A careful analysis of the involvement of vibrational sidelines can provide information about excitation delocalisation. An example is the observation of host modes in the luminescence spectra of naphthalene-d_x doped in naphthalene-d_8. This has been used[45] to estimate the extent of delocalisation of the lowest-energy excitation of naphthalene-d_x into the naphthalene-d_8 host.

A ligand centered π-π^* excitation in a complex couples strongly to the modes of the excited ligand, but only weakly to metal-ligand modes and modes of other (non-excited) ligands. Metal centered (d-d or f-f) excitations couple to metal-ligand modes and may couple quite strongly to ligand modes when the bonding to the ligand in the excited state changes.

Localised MLCT excitations need to be considered with particular care. These excitations are characteristically *two center* transitions. The neutral "spectator" ligands see the metal-core being reduced in the emission process

$$L^-\text{-}Ru^{3+}\text{-}L_2 \rightarrow L\text{-}Ru^{2+}\text{-}L_2 + h\nu. \qquad (8)$$

Sidelines associated with the spectator modes will couple to this process. It is well known that the backbonding interaction between Ru(II) and an imine π^* system is strong, but weak with Ru(III). Thus there will be a distinct change of metal-π^* interaction between ground and excited states. The appearance of spectator ligand vibrational sidelines in the luminescence spectrum cannot be used as evidence for delocalisation of ^{3}MLCT states.

In the luminescence of $[Ru(bpy)_2(bprid)]^{2+}$ in $[Zn(bpy)_3](ClO_4)_2$, the ^{3}MLCT state is localised on the bprid ligand,[24] yet vibrational sidelines due to the bpy ligands are observed over the entire frequency range. For example, the *most intense* sideline in the low frequency range is the 477 cm^{-1} bpy mode.[24]

Braun *et al.*[28] have reported studies on the related $[Ru(bpy)_2(bpz)]^{2+}$ system. They were not able to identify any sidebands associated with *high* frequency modes of the (spectator) bpy ligands. They claimed this absence to be a necessary consequence of localisation of the luminescent ^{3}MLCT state on the bpz. We have remeasured[46] this system with greater sensitivity and have been able to unambiguously identify bpy sidelines over the entire frequency range. It is important to note that in the bpz and bprid systems, the intensity of the origin

features (relative to the overall luminescence) are quite different from $[Ru(bpy)_3]^{2+}$. Spectra need to be scaled before any detailed comparison of sideline structures is made.

Figure 19 compares the sidelines in the luminescence spectra of the series $[Ru(bpy)_{3-x}(bpy\text{-}d_8)_x]^{2+}$ in $[Zn(bpy)_3](ClO_4)_2$. Both deuterated and protonated modes can be observed in the emission of the x = 1 system, although the lowest excited state is localised on a bpy-h_8 ligand. Similarly, both deuterated and protonated modes appear in the x = 2 system. Here emission originates either on the bpy-h_8 or the bpy-d_8 ligand. It is important to note that emission which occurs from bpy-d_8 shows substantially stronger coupling to deuterated modes than emission from bpy-h_8 and *vice versa.*

We have shown in Section 5.1 that the lowest-excited state in the $[Os(bpy)(bpy\text{-}d_8)_2]^{2+}$ complex doped into the $[Ru(bpy)_3](PF_6)_2$ host is localised on the bpy-h_8 ligand. Stronger coupling of vibrational sidelines associated with the bpy-h_8 in comparison with those due to the bpy-d_8 ligands is observed. The $\approx$480 cm^{-1} mode associated with the bpy-h_8 ligand is the most intense sideline feature in the x = 2 system.

The intensity of sideline patterns for the same chromophore in the two types of lattices studied are rather different. This sensitivity to environment provides a further caveat to the interpretation of sideband structures.

7. CONCLUSIONS

Our studies in high symmetry crystal lattices have allowed us to make elegant and detailed measurements of a variety of $[M(L)_{3-x}(L')_x]^{2+}$ chromophores at sites of C_3 and C_2 symmetries. When x = 1 or 2 the chromophores substitute in the single crystallographic site of the C2/c lattice in two distinct ways.

We have established that the lowest-excited ^{3}MLCT states in Ru(II) complexes are localised and that the effective interaction β between metal-ligand subunits is less than $\approx$0.5 cm^{-1} in all the systems investigated. As inhomogeneously broadened linewidths are of the order of 5 cm^{-1} ^{3}MLCT transitions to the individual ligands are independent. Intramolecular excitation energy transfer between crys-

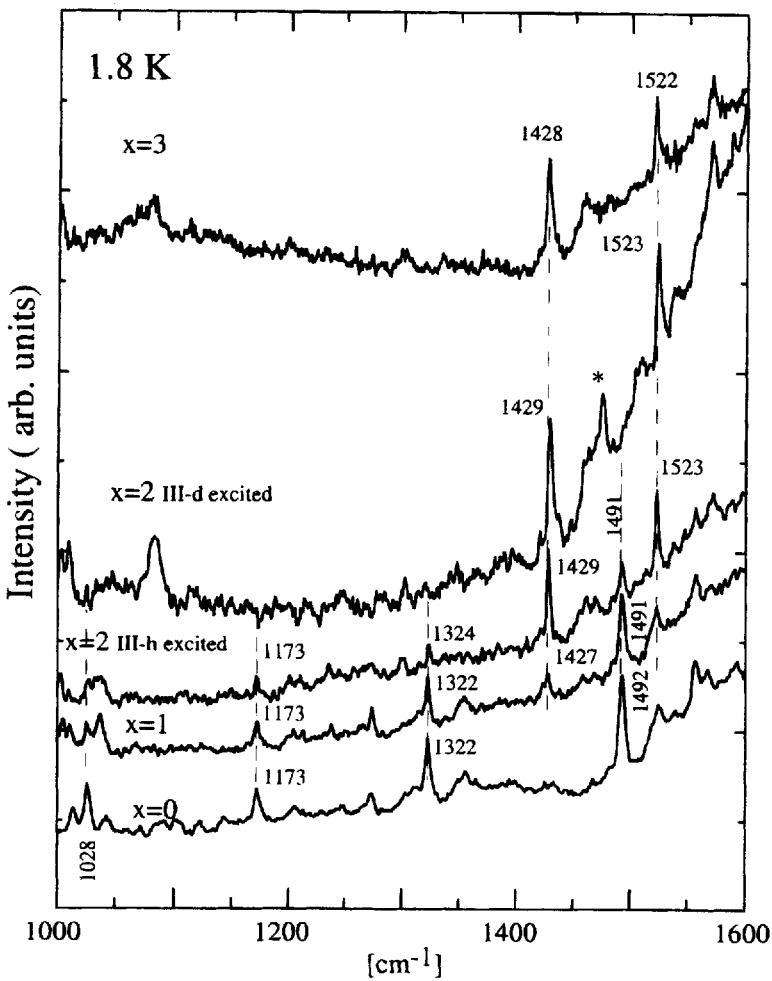

FIGURE 19 High frequency vibrational sidelines in the luminescence of the series $[Ru(bpy)_{3-x}(bpy\text{-}d_8)_x]^{2+}$ in $[Zn(bpy)_3](ClO_4)_2$. The asterisk in the II-d excited x = 2 spectrum denotes a sideline which is based upon I-h (I-h luminescence gets excited by intramolecular energy transfer and the background) (Ref. 24).

tallographically equivalent ligands occurs on a timescale of ≈10 ns in level II at lowest temperature.

The $[Os(bpy)_3]^{2+}$ complex shows an intramolecular exciton coupling which varies substantially between the $[Ru(bpy)_3](PF_6)_2$ (C_3) host and the $[M(bpy)_3](ClO_4)_2$ (M = Ru, Zn) (C_2) lattices. In the former lattice the effective excitation exchange interaction is $\beta = -2.3\ cm^{-1}$. This excitation exchange interaction leads to Davidov splittings which are comparable to the inhomogeneous width of the electronic origins. Thus the lowest-energy excitations are excitons involving all three ligands, although the coherence is low. Partial deuteration localises the lowest-excited exciton level on the protonated ligand(s) in the $[Os(bpy)_2(bpy\text{-}d_8)]^{2+}$ and $[Os(bpy)(bpy\text{-}d_8)_2]^{2+}$ complexes.

In the $[M(bpy)_3](ClO_4)_2$ (M = Ru,Zn) lattices, substantially larger excitation exchange interactions ($\beta \approx +30$ to $+80\ cm^{-1}$) are observed between the two crystallographically equivalent ligands, and thus partial deuteration cannot localise the exciton. The lowest-excited levels are excitons which involve both crystallographically equivalent ligands with higher coherence.

In solutions and glasses the effects of nanoheterogeneity ensure that the lowest-excited ^{3}MLCT states are invariably localised for both the Ru(II) and Os(II) diimine complexes.

Acknowledgments

We are grateful to Drs. L. Wallace and L. Dubicki and Mr. J. Kelly for their assistance. We would like to thank Professor D. P. Craig for his interest in this work. H.R. thanks the Australian Research Council for a Fellowship.

References

1. M. K. DeArmond and C. M. Carlin, Coord. Chem. Rev. **36**, 325 (1981).
2. K. Kalyanasundaram, Coord. Chem. Rev. **46**, 159 (1982).
3. T. J. Meyer, Prog. Inorg. Chem. **130**, 389 (1984).
4. J. Ferguson, F. Herren, E. R. Krausz, M. Maeder and J. Vrbanich, Coord. Chem. Rev. **64**, 21 (1985).
5. A. Juris, F. Barigelletti, S. Campagna, V. Balzani, P. Belser and A. von Zelewsky, Coord. Chem. Rev. **84**, 85 (1988).
6. E. Krausz and J. Ferguson, Prog. Inorg. Chem. **37**, 293 (1989).

7. P. G. Bradley, H. Kress, B. A. Hornberger, R. F. Dallinger and W. H. Woodruff, J. Am. Chem. Soc. **103**, 7441 (1981).
8. W. K. Smothers and M. S. Wrighton, J. Am. Chem. Soc. **105**, 1067 (1983).
9. A. Juris, F. Barigelleti, V. Balzani, P. Belser and A. Zelewsky, Inorg. Chem. **24**, 202 (1985).
10. M. Kato, S. Yamauchi and N. Hirota, J. Phys. Chem. **93**, 3422 (1989).
11. D. R. Striplin and G. A. Crosby, Chem. Phys. Lett. **221**, 426 (1994).
12. G. A. Heath, L. J. Yellowlees and P. S. Braterman, Chem. Phys. Lett. **92**, 646 (1982).
13. H. Riesen and E. Krausz, *Australian Conference on Lasers and Spectroscopy*, Abstract B49 (Gold Coast, Australia, 1987).
14. P. J. Caroll and L. E. Brus, J. Am. Chem. Soc. **109**, 7613 (1987).
15. D. P. Craig and S. H. Walmsley, *Excitons in Molecular Crystals*, (W. A. Benjamin Inc., New York, 1968).
16. A. H. Zewail, D. D. Smith and J.-P. Lemaistre, in *Excitons*, eds. E. I. Rashba and M. D. Sturge, p. 666 (North-Holland Publishing, 1982).
17. V. L. Broude, E. I. Rashba and E. F. Sheka, *Spectroscopy of Molecular Excitons*, Springer Series in Chemical Physics, Vol. 16 (Springer-Verlag, Berlin, 1985).
18. H. Riesen and E. Krausz, Comments Inorg. Chem. **14**, 323 (1993).
19. D. P. Rillema, D. S. Jones and H. A. Levy, J. Chem. Soc. Chem. Comm. 849 (1979).
20. M. Biner, H.-B. Bürgi, A. Ludi and C. Röhr, J. Am. Chem. Soc. **114**, 5197 (1992).
21. E. Krausz, H. Riesen and A. D. Rae, Aust. J. Chem. **48**, 929 (1995).
22. J. M. Harrowfield and A. N. Sobolev, Aust. J. Chem. **47**, 763 (1994).
23. H. Riesen, L. Wallace and E. Krausz, submitted.
24. H. Riesen, L. Wallace and E. Krausz, Chem. Phys., in press.
25. N. Kitamura, Y. Kawanishi and S. Tazuke, Chem. Phys. Lett. **97**, 103 (1983).
26. L. Wallace, H. Riesen and E. Krausz, to be published.
27. J. Schmidt, J. Wudy, P. Huber, H. Domel, D. Braun and H. Yersin, Int. J. Mod. Phys. B **7**, 403 (1993).
28. H. Riesen and E. Krausz, J. Chem. Phys. **99**, 7614 (1993).
29. D. Braun, P. Huber, J. Wudy, J. Schmidt and H. Yersin, J. Phys. Chem. **98**, 8044 (1994).
30. P. Huber and H. Yersin, J. Phys. Chem. **97**, 12705 (1993).
31. H. Riesen, Y. Gao and E. Krausz, Chem. Phys. Lett. **228**, 610 (1994).
32. H. Riesen, unpublished results.
33. H. Riesen, L. Wallace and E. Krausz, Phys. Chem., in press.
34. H. Riesen, E. Krausz and M. Puza, Chem. Phys. Lett. **151**, 65 (1988).
35. H. Riesen and E. Krausz, J. Lum. **58**, 176 (1994).
36. H. Riesen, A. D. Rae and E. Krausz, J. Luminescence **62**, 123 (1994).
37. H. Riesen and E. Krausz, Chem. Phys. Lett. **212**, 347 (1993).
38. H. Riesen and E. Krausz, Chem. Phys. Lett. **217**, 613 (1994).
39. E. Krausz, Chem. Phys. Lett. **135**, 249 (1987).
40. H. Riesen and E. Krausz, Chem. Phys. Lett. **151**, 71 (1988).
41. H. Riesen, L. Wallace and E. Krausz, Chem. Phys. Lett. **228**, 605 (1994). Note that the phen transitions in Fig. 4(c) of that work are incorrectly labelled. Correct labelling is shown in Fig. 14 of the present work.
42. D. Braun, E. Gallhuber, G. Hensler and H. Yersin, Mol. Phys. **67**, 417 (1989).

43. H. Riesen, L. Wallace and E. Krausz, J. Chem. Phys. **102**, 4823 (1995).
44. H. Riesen and E. Krausz, "Intramolecular energy transfer and excitation coupling in metal-to-ligand charge transfer (MLCT) excited states," in *Excitonic Processes in Condensed Matter*, ed. Jai Singh, p. 408, Proc. SPIE 2362 (Bellingham, WA, 1995)
45. F. W. Ochs, P. N. Prasad and R. Kopelman, Chem. Phys. **6**, 253 (1974).
46. H. Riesen, L. Wallace and E. Krausz, submitted.